Supplementary information for:

High-latitude precipitation as a driver of multicentennial variability of the AMOC in a climate model of intermediate complexity

Oliver Mehling[1*], Katinka Bellomo[1,2], Michela Angeloni[2,3], Claudia Pasquero[2,4] and Jost von Hardenberg[1,2]

[1]Department of Environment, Land and Infrastructure Engineering, Politecnico di Torino, Turin, Italy.
[2]Institute of Atmospheric Sciences and Climate, National Research Council of Italy, Turin, Italy.
[3]Department of Physics and Astronomy, Alma Mater Studiorum – Università di Bologna, Bologna, Italy.
[4]Department of Earth and Environmental Sciences, University of Milano – Bicocca, Milan, Italy.

*Corresponding author(s). E-mail(s): oliver.mehling@polito.it;

List of Figures

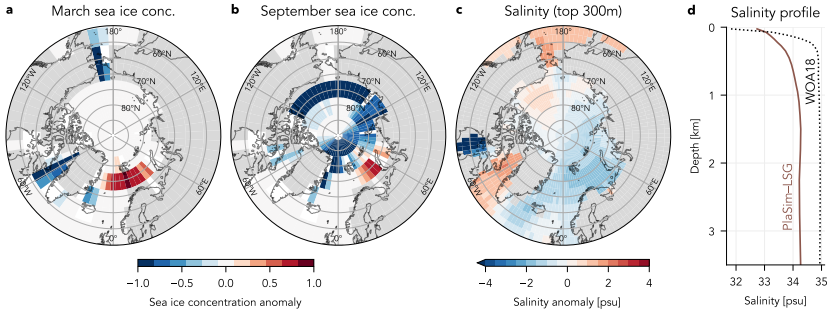

Fig. S1 Bias (simulated minus observed) for climatologies of (a) Arctic sea ice concentration in March, (b) Arctic sea ice concentration in September, (c) Annual mean salinity in the top 300 m. The sea ice climatology is computed from the HadISST dataset (Rayner et al, 2003) for the years 1870–1899 and the salinity climatology is obtained from the World Ocean Atlas 2018 (WOA18; Zweng et al, 2018). Before calculating biases, the observed climatologies are interpolated bilinearly to the resolution of PlaSim or LSG fields. (d) Mean salinity profile in the Arctic Ocean for the PlaSim–LSG control simulation and the WOA18 climatology.

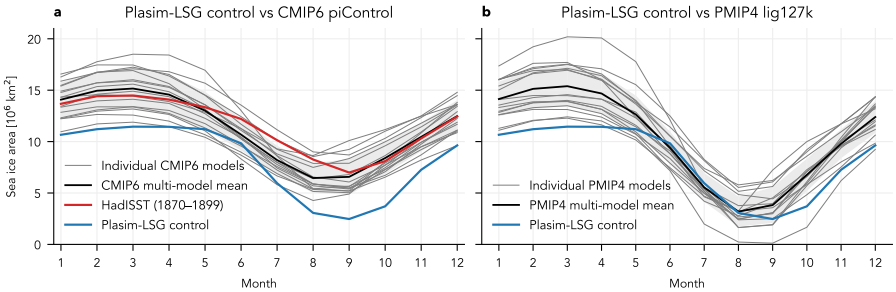

Fig. S2 Monthly climatology of Arctic sea ice area for the PlaSim–LSG control simulation compared to (a) *piControl* simulations of CMIP6 models and HadISST observations, (b) PMIP4 last interglacial (*lig127k*) simulations (Otto-Bliesner et al, 2021). Only CMIP6/PMIP4 models which ran both simulations are included in this plot. Light grey shading indicates one standard deviation around the CMIP6/PMIP4 multi-model means. See Figs. 4a and 4c of Otto-Bliesner et al (2021) for labels of the individual models.

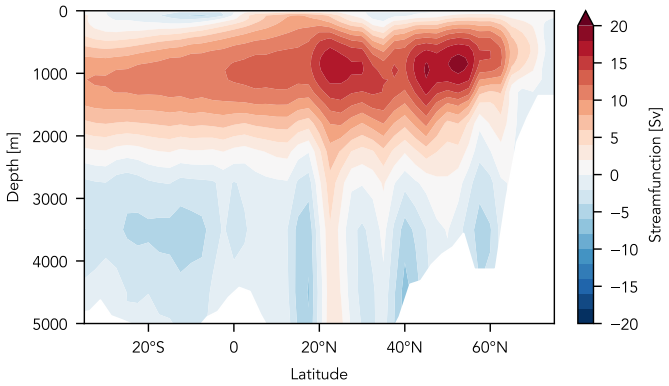

Fig. S3 Mean state of the Atlantic meridional overturning streamfunction in the control simulation.

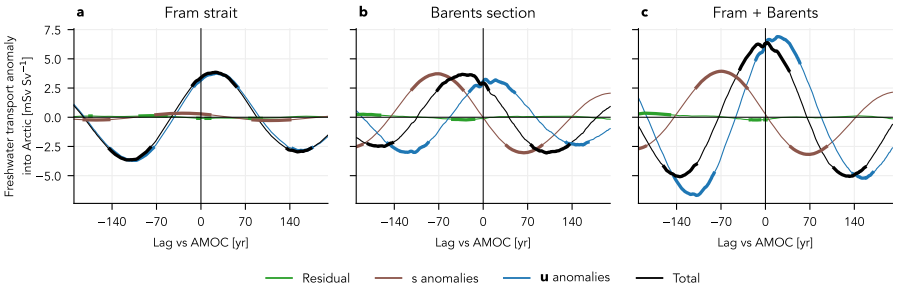

Fig. S4 Same as Fig. 5, but including the residual term (last term in Eq. 5).

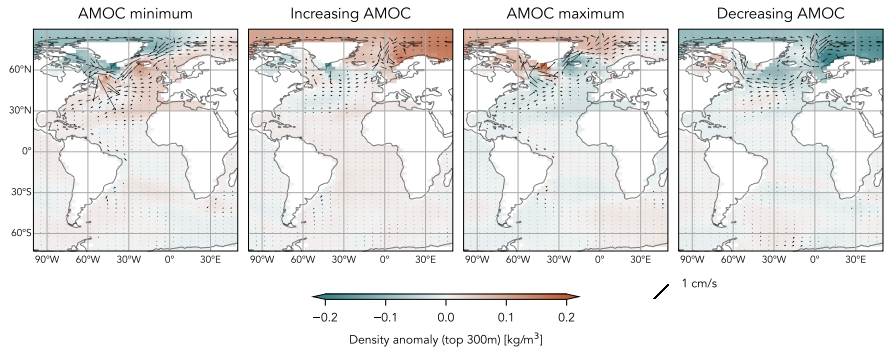

Fig. S5 Composites of density and velocity anomalies for four AMOC phases in the top 300m for the entire Atlantic basin.

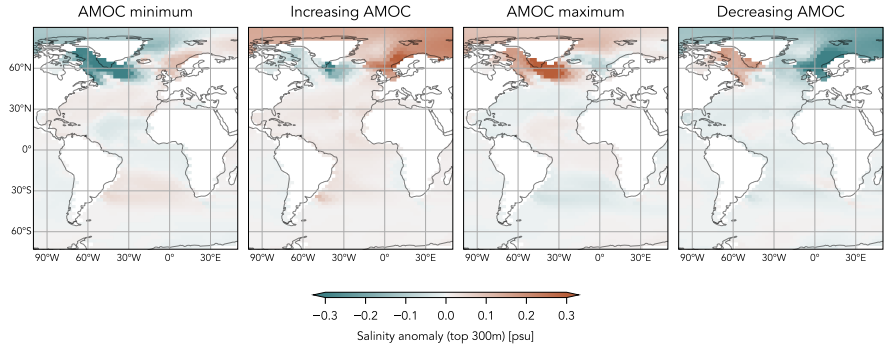

Fig. S6 Composites of salinity anomalies for four AMOC phases in the top 300m for the entire Atlantic basin.

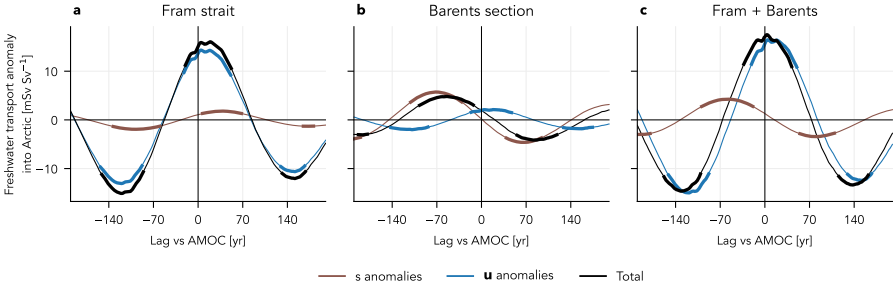

Fig. S7 Same as Fig. 5, but integrated over the full depth. Note that the scale of the y-axis differs from that of Fig. 5.

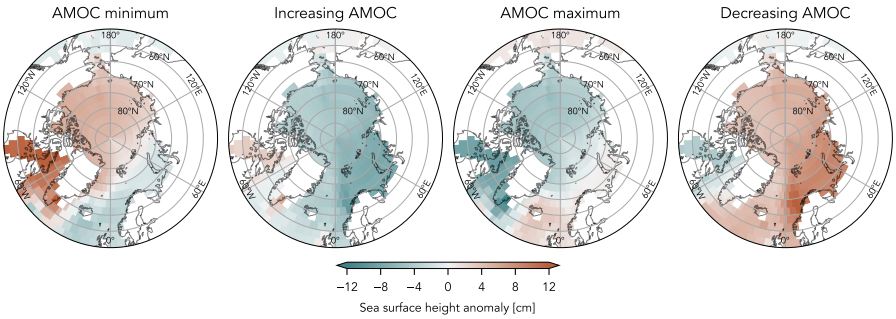

Fig. S8 Composites of sea surface height for four AMOC phases.

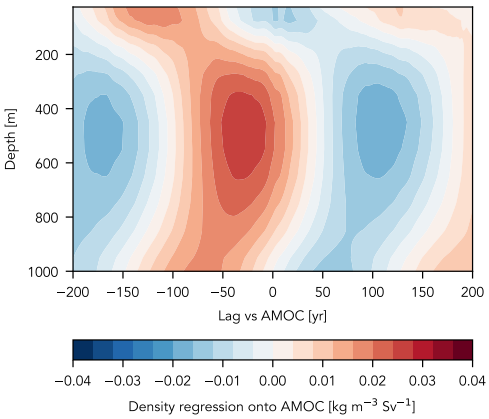

Fig. S9 Longitudinally averaged lag regression of ρ'_s onto AMOC strength in the Denmark strait (in LSG: 66°N, 30°–17.5°W).

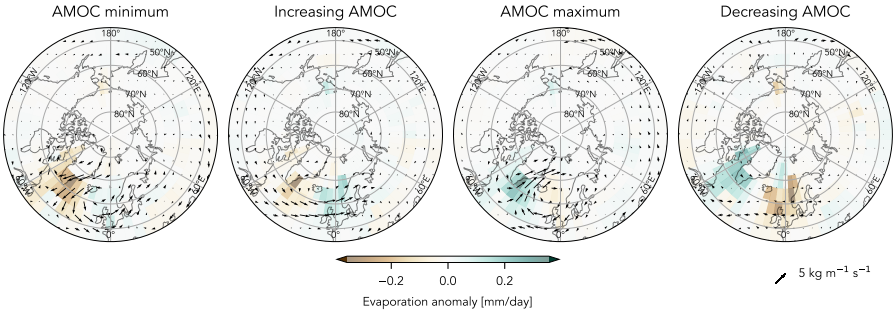

Fig. S10 Composites of evaporation anomalies (colors) and integrated moisture transport anomalies (arrows) for four AMOC phases. Integrated moisture transport is defined as $\mathbf{Q} = g^{-1} \int_0^{p_s} q\,\mathbf{u}\,\mathrm{d}p$, where $\mathbf{u}$ is the wind velocity, q is the specific humidity, and p_s is the surface pressure.

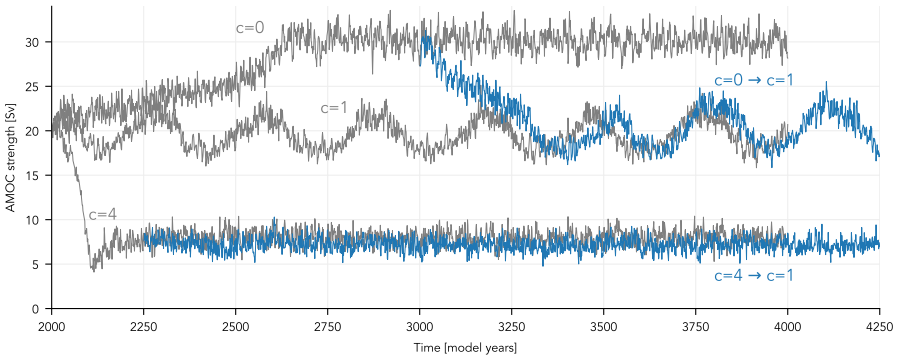

Fig. S11 Annual mean AMOC strength (40–60°N) for selected sensitivity experiments. The grey curves are identical to those for $c = \{0, 1, 4\}$ in Fig. 10. The blue curves correspond to simulations with c reset to 1. They were branched off from the $c = 0$ experiment at $t = 3000$ years and from the $c = 4$ experiment at $t = 2250$ years, after these experiments had approached their respective equilibrium state of the AMOC.

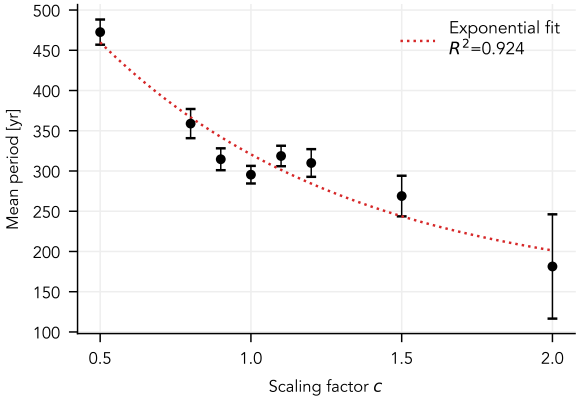

Fig. S12 Mean period of AMOC oscillations for sensitivity experiments with a scaling factor of $0.5 \leq c \leq 2$ as given by the first maximum of the autocorrelation function. Error bars show 95% confidence intervals estimated via a moving-block bootstrap resampling (block size 30 years) of the residuals after applying a 100-year running mean to the time series in Fig. 10.

Supplementary References:

Otto-Bliesner BL, Brady EC, Zhao A, et al (2021) Large-scale features of Last Interglacial climate: Results from evaluating the *lig127k* simulations for the Coupled Model Intercomparison Project (CMIP6)–Paleoclimate Modeling Intercomparison Project (PMIP4). Clim Past 17:63–94. https://doi.org/10.5194/cp-17-63-2021

Rayner NA, Parker DE, Horton EB, et al (2003) Global analyses of sea surface temperature, sea ice, and night marine air temperature since the late nineteenth century. J Geophys Res Atmospheres 108. https://doi.org/10.1029/2002JD002670

Zweng M, Seidov D, Boyer T, et al (2018) World Ocean Atlas 2018, Volume 2: Salinity. NOAA Atlas NESDIS 82